Photoionization and recombination of a hydrogen atom in a magnetic field

O. Chuluunbaatar,[1] A. A. Gusev,[1] S. I. Vinitsky,[1] V. L. Derbov,[2] L. A. Melnikov,[2] and V. V. Serov[2]
[1]*Joint Institute for Nuclear Research, Dubna, Russia*
[2]*Saratov State University, Saratov, 410012, Russia*
(Received 18 December 2007; published 21 March 2008)

Application of the adiabatic method and program packages for solving the boundary problem for a discrete and continuous spectrum of a hydrogenlike atom in a homogeneous magnetic field is presented. Based on this the estimation of the photoionization cross section and laser-induced recombination rate is carried out. Effects of resonance transmission and total reflection of oppositely charged particles in a homogeneous magnetic field are demonstrated.

DOI: 10.1103/PhysRevA.77.034702 PACS number(s): 32.80.Fb

In a recent paper [1] an alternative mechanism of laser-induced recombination of antihydrogen from cold antiproton-positron plasma in a magnetic trap was revealed. This resonance mechanism makes use of quasistationary states embedded in the continuum. These states arise due to the transverse confinement potential induced by the magnetic field. The optimization of laser and magnetic field parameters in the case when the Coulomb energy is comparable with that of the magnetic field can be studied by means of the adiabatic approach in spherical coordinates using the basis of angular oblate spheroidal functions [2]. An attractive feature of this approach is that the electron wave function is accurately evaluated near the origin irrespective of the field strength [3,4]. However, the key point for the scattering problem is how to match the spherically symmetric wave functions near the origin with the wave functions possessing the cylindrical symmetry which are more appropriate in the area located far enough from the origin [5]. This problem was resolved in the appropriate calculation scheme and program packages aimed at the solution of the boundary problems for discrete and continuous spectrum of a hydrogenlike atom in a homogeneous magnetic field developed by the authors earlier [6–8].

In this Brief Report we apply this approach to the calculation of the optical transitions between the bound and the autoionization states both of discrete and continuous spectrum. Our analysis revealed the effects of resonance transmission and total reflection of oppositely charged particles in a homogeneous magnetic field related to the existence of quasistationary states embedded in the continuum.

The Schrödinger equation for the wave function $\hat{\Psi}(\Omega)=\Psi(r,\eta)\exp(\imath m\varphi)/\sqrt{2\pi}$ of a hydrogen atom with the charge Z of the nucleus in the axially symmetric magnetic field $\mathbf{B}=(B_x=0,B_y=0,B_z=B)$ written in spherical coordinates $\Omega=(r,\eta=\cos\theta,\varphi)$ is reduced to the two-dimensional (2D) equation for the partial component $\Psi(r,\eta)\equiv\Psi^{m\sigma}(r,\eta)=\sigma\Psi^{m\sigma}(r,-\eta)$ at fixed values of the magnetic quantum number $m=0,\pm1,\ldots$ and z parity $\sigma=\pm1$,

$$\left(-\frac{1}{r^2}\frac{\partial}{\partial r}r^2\frac{\partial}{\partial r}+\frac{1}{r^2}\hat{A}(p)-\frac{2Z}{r}\right)\Psi(r,\eta)=\epsilon\Psi(r,\eta). \quad (1)$$

Here we use the atomic units (a.u.) $\hbar=m_e=e=1$ and put the mass of the nucleus to be infinite, $\epsilon=2E$, E is the energy [expressed in Rydbergs, 1 Ry=(1/2) a.u.] of the state $|m\sigma\rangle$. The operator $\hat{A}(p)$ is defined by

$$\hat{A}(p)=-\frac{\partial}{\partial\eta}(1-\eta^2)\frac{\partial}{\partial\eta}+\frac{m^2}{1-\eta^2}+2pm+p^2(1-\eta^2),$$

where $p=\gamma r^2/2$ is the confinement potential induced by the magnetic field, $\gamma=B/B_0$ is a dimensionless parameter determined by the field B, and $B_0\cong2.35\times10^5$ T.

Let us consider a formal adiabatic expansion of the partial solution $\Psi_i^{Em\sigma}(r,\eta)$ of Eq. (1) in terms of one-dimensional basis functions $\{\Phi_j^{m\sigma}(\eta;r)\}_{j=1}^{j_{\max}}$,

$$\Psi_i^{Em\sigma}(r,\eta)=\sum_{j=1}^{j_{\max}}\Phi_j^{m\sigma}(\eta;r)\chi_j^{(m\sigma i)}(E,r). \quad (2)$$

The radial wave functions $\boldsymbol{\chi}^{(i)}(r)\equiv\boldsymbol{\chi}^{(m\sigma i)}(E,r)$, $[\boldsymbol{\chi}^{(i)}(r)]^T=(\chi_1^{(i)}(r),\ldots,\chi_{j_{\max}}^{(i)}(r))$ are unknown, the orthonormal basis wave functions $\Phi_j(r,\eta)\equiv\Phi_j^{m\sigma}(\eta;r)=\sigma\Phi_j^{m\sigma}(-\eta;r)$ and the potential curves $E_j(r)$ (in Ry) are the solutions of the parametric eigenvalue problem

$$\hat{A}(p)\Phi_j(\eta;r)=E_j(r)\Phi_j(\eta;r). \quad (3)$$

The solutions of this problem with shifted eigenvalues $\check{E}_j(r)=E_j(r)-2pm$ correspond to the angular oblate spheroidal functions [9].

By using the expansion (2) we reduce the initial problem (1) to a boundary problem for a set of $j_{\max}$ coupled second-order ordinary differential equations that determine the radial wave functions $\boldsymbol{\chi}^{(i)}(r)$ of the expansion (2) in the finite interval $r\in[0,r_{\max}]$,

$$\left(-\frac{1}{r^2}\mathbf{I}\frac{d}{dr}r^2\frac{d}{dr}+\frac{\mathbf{U}(r)}{r^2}+\mathbf{Q}(r)\frac{d}{dr}+\frac{1}{r^2}\frac{dr^2\mathbf{Q}(r)}{dr}\right)\boldsymbol{\chi}^{(i)}(r)=\epsilon_i\mathbf{I}\boldsymbol{\chi}^{(i)}(r), \quad (4)$$

with the boundary condition at $r=0$,

$$\lim_{r\to0}r^2\left(\frac{d\boldsymbol{\chi}^{(i)}(r)}{dr}-\mathbf{Q}(r)\boldsymbol{\chi}^{(i)}(r)\right)=0. \quad (5)$$

Here $\mathbf{I}$, $\mathbf{U}(r)$, and $\mathbf{Q}(r)$ are $j_{\max}\times j_{\max}$ matrices with the elements

$$U_{ij}(r)=\frac{E_i(r)+E_j(r)-4Zr}{2}\delta_{ij}+r^2H_{ij}(r),\ \ I_{ij}=\delta_{ij},$$

$$H_{ij}(r) = H_{ji}(r) = \int_{-1}^{1} \frac{\partial \Phi_i(\eta;r)}{\partial r} \frac{\partial \Phi_j(\eta;r)}{\partial r} d\eta,$$

$$Q_{ij}(r) = -Q_{ji}(r) = -\int_{-1}^{1} \Phi_i(\eta;r) \frac{\partial \Phi_j(\eta;r)}{\partial r} d\eta, \quad (6)$$

where δ_{ij} is the Kronecker symbol. The eigenfunctions $\Phi_j(\eta;r)$, potential curves $E_j(r)$, and radial coupling matrix elements $H_{ij}(r)$ and $Q_{ij}(r)$ were calculated using the program POTHMF [8].

The discrete spectrum solutions $\boldsymbol{\chi}^{(i)}(r)$ obey the first-type boundary condition, $\boldsymbol{\chi}^{(i)}(r_{\max})=0$, which makes it possible to calculate the energy eigenvalues $E \equiv E_{m\sigma i\mathrm{v}}, \mathrm{v}=0, \mathrm{v}_{\max}$ and the corresponding eigenfunctions $\Psi_{i\mathrm{v}}^{m\sigma}(r,\eta) \equiv \Psi_i^{Em\sigma}(r,\eta)$ of Eq. (2) at $i=1$ using the program KANTBP [7]. The orthogonality and normalization condition for $\hat{\Psi}_{i\mathrm{v}}^{m\sigma}(\Omega)$ is

$$\langle \hat{\Psi}_{i\mathrm{v}}^{m\sigma}(\Omega) | \hat{\Psi}_{i'\mathrm{v}'}^{m'\sigma'}(\Omega) \rangle = \delta_{\mathrm{v}\mathrm{v}'} \delta_{mm'} \delta_{\sigma\sigma'} \delta_{ii'}. \quad (7)$$

The continuous-spectrum solutions $\boldsymbol{\chi}^{(i)}(r)$ obey the third-type boundary condition at fixed energy $\epsilon=2E$ above the first Landau threshold $E_j(\infty) \equiv \epsilon_{mj}^{th}(\gamma) = \gamma(2j-1+m+|m|)$ with $j=1$,

$$\frac{d\boldsymbol{\chi}(r)}{dr} = \mathbf{R}\boldsymbol{\chi}(r), \quad r = r_{\max}, \quad (8)$$

where $\mathbf{R}$ is a nonsymmetric $j_{\max} \times j_{\max}$ matrix which was calculated using the program KANTBP [7]. The orthogonality and normalization condition for $\hat{\Psi}_i^{Em\sigma}(\Omega)$ is

$$\langle \hat{\Psi}_i^{Em\sigma}(\Omega) | \hat{\Psi}_{i'}^{E'm'\sigma'}(\Omega) \rangle = \delta(E-E') \delta_{mm'} \delta_{\sigma\sigma'} \delta_{ii'}. \quad (9)$$

We express the corresponding eigenfunction $\Psi_i^{Em\sigma}(r,\eta)$ of the continuous spectrum with the energy $\epsilon=2E$ in open channels, $i=\overline{1,N_o}$, $N_o=\max_{2E\geq\epsilon_{mj}^{th}} j<j_{\max}$, in the form of Eq. (2), where $\hat{\boldsymbol{\chi}}^{(m\sigma)}(E,r) \equiv \{\boldsymbol{\chi}^{(i_o)}(r)\}_{i_o=1}^{N_o}$ is now the radial part of the eigenchannel or "incoming" wave function. The eigenchannel wave function $\hat{\boldsymbol{\chi}}^{(m\sigma)}(E,r)$ is expressed as

$$\hat{\boldsymbol{\chi}}^{(m\sigma)}(E,r) = (2/\pi)^{1/2} \boldsymbol{\chi}^{(p)}(r) \mathbf{C} \cos \boldsymbol{\delta}. \quad (10)$$

The function $\boldsymbol{\chi}^{(p)}(r)$ is a numerical solution of Eq. (4) that satisfies the "standing-wave" boundary conditions (8) and has the standard asymptotic form [7]

$$\boldsymbol{\chi}^{(p)}(r) = \boldsymbol{\chi}^{s}(r) + \boldsymbol{\chi}^{c}(r)\mathbf{K}, \quad \mathbf{KC} = \mathbf{C} \tan \boldsymbol{\delta}. \quad (11)$$

Here $\mathbf{K} \equiv \mathbf{K}_\sigma$ is the symmetric numerical *short-range reaction matrix* with the diagonal eigenvalue matrix $\tan \boldsymbol{\delta} \equiv \{\delta_{ij} \tan \delta_j\}_{ij=1}^{N_o}$ depending on the *short-range even or odd phase shift vector* $\boldsymbol{\delta} \equiv \boldsymbol{\delta}_\sigma = \{\delta_j^\sigma\}_{j=1}^{N_o}$, and the orthogonal matrix $\mathbf{C}^T\mathbf{C} = \mathbf{I}_{oo}$ of the corresponding eigenvectors $\mathbf{C}$, where $\mathbf{I}_{oo}$ is the unit $N_o \times N_o$ matrix. Note that in Eq. (10) $\cos \boldsymbol{\delta}$ is the diagonal matrix defined in the same terms. The regular $\boldsymbol{\chi}^s(r) = 2\,\mathrm{Im}[\boldsymbol{\chi}(r)]$ and irregular $\boldsymbol{\chi}^c(r) = 2\,\mathrm{Re}[\boldsymbol{\chi}(r)]$ asymptotic functions are expressed via the fundamental asymptotic solution $\boldsymbol{\chi}(r)$ with the leading terms at $r \to \infty$,

$$\chi_{ji_o}(r) = \frac{\exp[\imath p_{i_o} r + \imath\zeta \ln(2p_{i_o} r) + \imath\delta_{i_o}^c]}{2r\sqrt{p_{i_o}}} \delta_{ji_o}, \quad (12)$$

where p_{i_o} is the relative momentum in the channel i_o, $\zeta \equiv \zeta_{i_o} = Z/p_{i_o}$ is a Sommerfeld-type parameter, $\delta_{i_o}^c = \arg\Gamma(1-\imath\zeta)$ is the known Coulomb phase shift [9]. Using $\mathbf{R}$-matrix calculus [7], we obtain the equation expressing the reaction matrix $\mathbf{K}$ via the matrix $\mathbf{R}$ at $r=r_{\max}$,

$$\mathbf{K} = -\mathbf{X}^{-1}(r_{\max})\mathbf{Y}(r_{\max}), \quad (13)$$

where $\mathbf{X}(r)$ and $\mathbf{Y}(r)$ are square $N_o \times N_o$ matrices depending on the open-open matrix (channels)

$$\mathbf{X}(r) = \left(\frac{d\boldsymbol{\chi}^c(r)}{dr} - \mathbf{R}\boldsymbol{\chi}^c(r) \right)_{oo},$$

$$\mathbf{Y}(r) = \left(\frac{d\boldsymbol{\chi}^s(r)}{dr} - \mathbf{R}\boldsymbol{\chi}^s(r) \right)_{oo}. \quad (14)$$

The radial part of the "incoming" wave function $\hat{\boldsymbol{\chi}}^{(m\sigma)}(E,r) = (2/\pi)^{1/2}\boldsymbol{\chi}^-(r)$ is expressed via the numerical "standing" wave function and the short-range reaction matrix $\mathbf{K}$ by the relation

$$\boldsymbol{\chi}^-(r) = \imath\boldsymbol{\chi}^{(p)}(r)(\mathbf{I}_{oo} + \imath\mathbf{K})^{-1} \quad (15)$$

and has the asymptotic form

$$\hat{\boldsymbol{\chi}}^{(m\sigma)}(E,r) = (2/\pi)^{1/2}[\boldsymbol{\chi}(r) - \boldsymbol{\chi}^*(r)\mathbf{S}^\dagger]. \quad (16)$$

Here $\mathbf{S} \equiv \mathbf{S}_\sigma$ is the unitary short-range scattering matrix, $\mathbf{S}^\dagger\mathbf{S} = \mathbf{S}\mathbf{S}^\dagger = \mathbf{I}_{oo}$, which can be expressed via the calculated $\mathbf{K}$ matrix as

$$\mathbf{S} = (\mathbf{I}_{oo} + \imath\mathbf{K})(\mathbf{I}_{oo} - \imath\mathbf{K})^{-1}. \quad (17)$$

The ionization wave function $\boldsymbol{\Psi}_{Em\hat{v}}^{(-)}(r,\eta) \equiv \boldsymbol{\Psi}_{Em\rightleftarrows}^{(-)}(r,\eta)$ has the asymptotic form reverse to the common scattering problem, namely, "incident wave+ingoing wave"

$$\boldsymbol{\Psi}_{Em\hat{v}}^{(-)}(r,\eta) = \frac{\boldsymbol{\Psi}^{Em,+1}(r,\eta) \pm \boldsymbol{\Psi}^{Em,-1}(r,\eta)}{\sqrt{2}} \exp(-\imath\boldsymbol{\delta}^c). \quad (18)$$

The function $\boldsymbol{\Psi}_{Em\hat{v}}^{(-)}(r,\eta)$ corresponds to the function $|E\hat{v}mN_\rho\rangle$ defined in the cylindrical coordinates (ρ,z,φ),

$$|E\hat{v}mN_\rho\rangle = \frac{\exp(\imath m\varphi)}{2\pi} \sum_{n'=1}^{j_{\max}} \Phi_{n'}(\rho) \chi_{Em\hat{v}n'n}^{(-)}(z). \quad (19)$$

Here $N_\rho = n-1$, $\hat{v}$ denotes the initial direction of the particle motion along the z axis, and $\Phi_{n'}(\rho)$ is the eigenfunction of a two-dimensional oscillator that corresponds to $\Phi_j^{m\hat{v}}(r,\eta) = [\Phi_j^{m,+1}(r,\eta) \pm \Phi_j^{m,-1}(r,\eta)]/\sqrt{2}$ at $r \to \infty$. At $z \to \pm\infty$ the function $\chi_{Em\hat{v}n'n}^{(-)}(z)$ has the following asymptotic form:

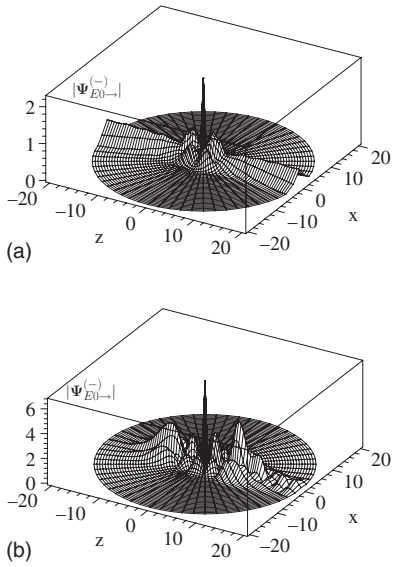

FIG. 1. Profiles $|\Psi^{(-)}_{Em\rightarrow}|$ of the total wave function (18) in the zx plane with $Z=1$, $m=0$, $\gamma=0.1$ and the energies $E=0.058\ 85$ a.u. (a) and $E=0.116\ 92$ a.u. (b), demonstrating resonance transmission and total reflection, respectively.

$$\chi^{(-)}_{E\upsilon}(z)=\begin{cases}\mathbf{X}^{(+)}(z)+\mathbf{X}^{(-)}(z)\hat{\mathbf{R}}^{\dagger}, & z>0,\\ \mathbf{X}^{(+)}(z)\hat{\mathbf{T}}^{\dagger}, & z<0,\end{cases}\quad \hat{\upsilon}=\rightarrow,$$

$$\begin{cases}\mathbf{X}^{(-)}(z)\hat{\mathbf{T}}^{\dagger}, & z>0,\\ \mathbf{X}^{(-)}(z)+\mathbf{X}^{(+)}(z)\hat{\mathbf{R}}^{\dagger}, & z<0,\end{cases}\quad \hat{\upsilon}=\leftarrow, \tag{20}$$

where the matrix elements of $\mathbf{X}^{(\pm)}(z)$ are

$$X^{(\pm)}_{n'n}(z)=\exp\left(\pm\imath p_{n'}z\pm\imath\zeta_{n'}\frac{z}{|z|}\ln(2p_{n'}|z|)\right)\frac{\delta_{n'n}}{\sqrt{p_{n'}}}, \tag{21}$$

$\hat{\mathbf{T}}$ and $\hat{\mathbf{R}}$ are the transmission and reflection amplitude matrices, $\hat{\mathbf{T}}^{\dagger}\hat{\mathbf{T}}+\hat{\mathbf{R}}^{\dagger}\hat{\mathbf{R}}=\mathbf{I}_{oo}$. It is easy to show that $\hat{\mathbf{T}}$ and $\hat{\mathbf{R}}$ may be expressed in terms of the long-range scattering matrices $\check{\mathbf{S}}_{\sigma}=\exp(\imath\boldsymbol{\delta}^{\sigma})\mathbf{S}_{\sigma}\exp(\imath\boldsymbol{\delta}^{\sigma})$ as

$$\hat{\mathbf{T}}=2^{-1}(-\check{\mathbf{S}}_{+1}+\check{\mathbf{S}}_{-1}),$$

$$\hat{\mathbf{R}}=2^{-1}(-\check{\mathbf{S}}_{+1}-\check{\mathbf{S}}_{-1}). \tag{22}$$

Therefore the cross section $\sigma^{d}_{Nlm}(\omega)$ of photoionization of the atom by the light, linearly polarized along the axis z, is expressed as

$$\sigma^{d}_{Nlm}(\omega)=4\pi^2\alpha\omega\sum_{i=1}^{N_o}|D^{m\sigma\sigma'}_{i,N,l}(E)|^2a_0^2, \tag{23}$$

where α is the fine-structure constant, a_0 is the Bohr radius, and $D^{m\sigma\sigma'}_{i,N,l}(E)\equiv D^{m\sigma\sigma'}_{i,i',\nu'}(E)$ are the dipole moment matrix elements

$$D^{m\sigma\sigma'}_{i,i',\nu'}(E)=\langle\Psi^{Em\sigma=\mp1}_{i}(r,\eta)|r\eta|\Psi^{m\sigma'=\pm1}_{i'\nu'}(r,\eta)\rangle. \tag{24}$$

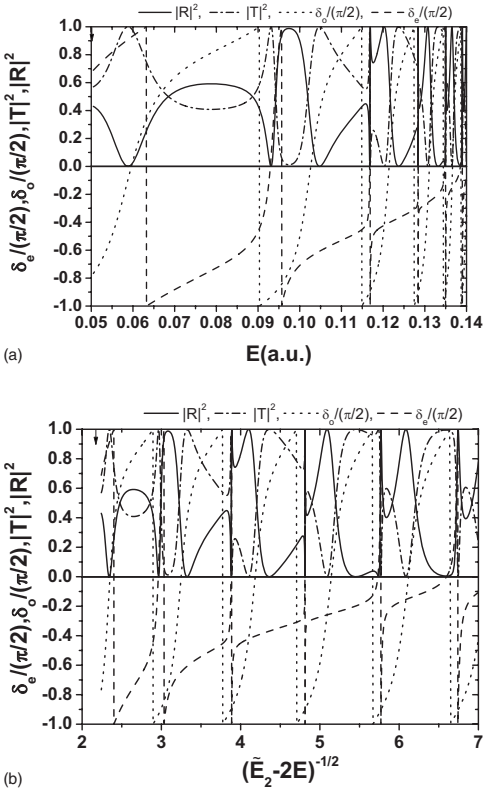

FIG. 2. Transmission $|\hat{\mathbf{T}}|^2$ and reflection $|\hat{\mathbf{R}}|^2$ coefficient (22), even δ_e and odd δ_o short-range phase shifts (11) versus the energy E (a) and $(\tilde{E}_2-2E)^{-1/2}$ (b) for $Z=1$, $m=0$, $\gamma=0.1$. Arrow marks the first threshold $E_1=\gamma/2$.

In the above expressions $\omega=E-E_{Nlm}$ is the frequency of radiation and $E_{Nlm}\equiv E_{m\sigma' i'\nu'}$ is the energy of the initial bound state $|Nlm\rangle=\Psi^{m\sigma'}_{i'\nu'}(r,\eta)$ below the first threshold shift $\epsilon^{th}_{m1}(\gamma)/2$ at $i'=1$. The continuous spectrum solution $\boldsymbol{\chi}^{(p)}(r)$ having the asymptotic form of a "standing" wave and the reaction matrix $\mathbf{K}$ required for using Eq. (10) or Eq. (16), as well as the discrete spectrum solution $\boldsymbol{\chi}(r)$ and the eigenvalue $E_{m\sigma' i'=1\nu'}$, were calculated using the program KANTBP [7].

Profiles of the wave function (18) for $Z=1$, $m=0$, $\gamma=0.1$, $j_{\max}=10$, and $N_o=1$ are shown in Fig. 1 at two fixed values of energy E, corresponding to resonance transmission $|\hat{\mathbf{T}}|^2=\sin^2(\delta_e-\delta_o)=1$ and total reflection $|\hat{\mathbf{R}}|^2=\cos^2(\delta_e-\delta_o)=1$. Here $\delta_e\equiv\delta_1^{+1}$ and $\delta_o\equiv\delta_1^{-1}$ are the *short-range phase shifts* for even and odd states from Eq. (11), respectively. The transmission and reflection coefficients are explicitly shown in Fig. 2 together with the even δ_e and odd δ_o phase shifts versus the energy E [Fig. 2(a)] and $(\tilde{E}_2-2E)^{-1/2}$ [Fig. 2(b)], where $\tilde{E}_2=\epsilon^{th}_{m2}(\gamma)$ is the second threshold shift. The quasistationary states imbedded in the continuum correspond to the *short-range phase shifts* $\delta_{o(e)}=n_{o(e)}\pi+\pi/2$ at $(\tilde{E}_2-2E)^{-1/2}=n_{o(e)}+\Delta_{n_{o(e)}}$. Nonmonotonic behavior of $|\hat{\mathbf{T}}|$ and $|\hat{\mathbf{R}}|$ is seen to include the cases of resonance transmission and total reflection, related to the existence of these quasistationary states.

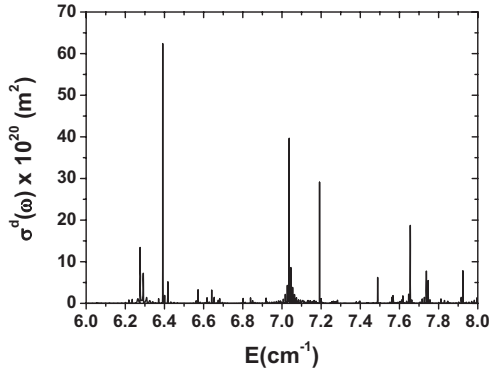

FIG. 3. Cross section of photoionization from the state $3s_0$ versus the energy E for $\gamma=2.595\times10^{-5}$ and the final state with $\sigma=-1$, $Z=1$, $m=0$.

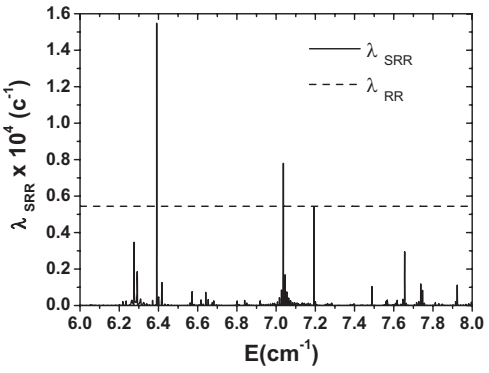

FIG. 4. Laser-stimulated radiative recombination rate into the bound state $N'=3$, $l'=0$, $m'=0$ versus the energy E of the initially free positron.

Figure 3 clarifies the behavior of the cross section of photoionization by the light, linearly polarized along the axis z, from the rotational state $3s_0$ at $B_0=6.1$ T ($\gamma=2.595\times10^{-5}$) in the energy interval $E=6.0-8.0$ cm^{-1} at $j_{\max}=35$. The cross sections have been calculated with the energy step 5×10^{-4} cm^{-1} in all the regions except the vicinity of peaks, where the step was 5×10^{-6} cm^{-1}. From our numerical experiments it follows that the absolute maximal values of the continuum wave functions $\hat{\chi}^{(01)}_{j1}(E,r)$ decrease from 10^{-4} to 10^{-6} when the number of components j is increased from 30 to 35, thus demonstrating the linear rate of convergence of the expansion (2) in the energy interval considered. The relation between the photoionization cross section and the induced radiative recombination rate [1] makes it possible to apply the above results to the urgent problem of production of cold antihydrogen atoms in magnetic traps [10].

As an example, consider the recombination into the state $N'=3$, $l'=0$, $m'=0$ that may be stimulated by a titanium-sapphire laser, under the conditions typical for positron-antiproton plasma in magnetic traps used for antihydrogen production, namely, the temperature of the plasma $T=4$ K, the positron density $n_e=1\times10^8$ cm^{-3}, and the magnetic induction $B=6.10$ T. The laser intensity is taken such that at 4 K without the magnetic field the rate of induced recombination is equal to that of the spontaneous one. In particular, for $N=3$ this intensity is $I=24$ W/cm^2 [11]. Figure 4(b) shows the dependence of the laser-stimulated recombination rate λ_{SRR} per one antiproton upon the initial energy $E=E_{Nlm}+\omega$ of the positron. For comparison the horizontal dashed line displays the rate λ_{RR} of the spontaneous radiative recombination into all the states with $N=3$, which at the intensity considered is equal to the rate of the laser-stimulated recombination without the magnetic field [11]. One can see narrow resonances for which the rate of recombination into the state with fixed $l=0$, $m=0$ in the magnetic field is appreciably higher than the rate of recombination into all nine states with different l and m possible for $N=3$ without the magnetic field. Thus we demonstrated the efficiency of the proposed approach and program packages in calculations of photoionization and laser-induced recombination of a (anti)hydrogen atom in the magnetic field and the effects of resonance transmission and total reflection of oppositely charged particles in the magnetic field.

Further applications of the method may be associated with calculations of laser-induced recombination of antihydrogen in magnetic traps [1,6], channeling of light nuclei in thin doped films [12], and potential scattering with confinement potentials [13].

The authors thank Professor A.G. Abrashkevich, Professor A. M. Ermolaev, Professor V. S. Melezhik, Professor M. S. Kaschiev, and Professor V. V. Pupyshev for useful discussions. This work was partly supported by Grants No. CRDF BRHE REC-006 SR-006-X1/B75M06 Y3-P-06-08 and No. 07-01-00660, and JINR theme 09-6-1060-2005/2009.

[1] V. V. Serov *et al.*, Opt. Spectrosc. **102**, 557 (2007).
[2] U. Fano, Colloq. Int. C. N. R. S. **273**, 127 (1977); A. F. Starace and G. L. Webster, Phys. Rev. A **19**, 1629 (1979).
[3] M. S. Kaschiev, S. I. Vinitsky, and F. R. Vukajlovic, Phys. Rev. A **22**, 557 (1980).
[4] M. G. Dimova, M. S. Kaschiev, and S. I. Vinitsky, J. Phys. B **38**, 2337 (2005).
[5] C. V. Clark, K. T. Lu, and A. F. Starace, in *Progress in Atomic Spectroscopy, Part C*, edited by H. G. Beyer and H. Kleinpoppen (Plenum, New York, 1984), p. 247.
[6] O. Chuluunbaatar *et al.*, J. Phys. A **40**, 11485 (2007).
[7] O. Chuluunbaatar *et al.*, Comput. Phys. Commun. **177**, 649 (2007).
[8] O. Chuluunbaatar *et al.*, Comput. Phys. Commun. **178**, 301 (2008).
[9] M. Abramovits and I. A. Stegun, *Handbook of Mathematical Functions* (Dover, New York, 1972).
[10] L. I. Men'shikov and R. Landua, Phys. Usp. **46**, 227 (2003).
[11] M. V. Ryabinina and L. A. Melnikov, Nucl. Instrum. Methods Phys. Res. B **214**, 35 (2004).
[12] Yu. N. Demkov and J. D. Meyer, Eur. Phys. J. B **42**, 361 (2004).
[13] J. I. Kim, V. S. Melezhik, and P. Schmelcher, Phys. Rev. Lett. **97**, 193203 (2006).